Giant Magnon-Driven Magnetothermal Transport in Magnetic Multilayers

Ping Tang[1],* Ken-ichi Uchida[2,3], and Gerrit E. W. Bauer[1,4,5]
[1] *WPI-AIMR, Tohoku University, Sendai 980-8577, Japan*
[2] *National Institute for Materials Science (NIMS), Tsukuba 305-0047, Japan*
[3] *Department of Advanced Materials Science, Graduate School of Frontier Sciences, The University of Tokyo, Kashiwa 277-8561, Japan*
[4] *Institute for Materials Research and CSIS, Tohoku University, Sendai 980-8577, Japan and*
[5] *Kavli Institute for Theoretical Sciences, University of the Chinese Academy of Sciences, Beijing 10090, China*
(Dated: April 28, 2025)

All-solid-state nanoscale devices capable of efficiently controlling a heat flow are crucial for advanced thermal management technologies. Here we predict a magnon-driven magnetothermal resistance (mMTR) effect in multilayers of ferromagnets and normal metals, i.e. a thermal resistance that varies when switching between parallel and antiparallel magnetization orientations of the ferromagnetic layers, even in the absence of conduction electrons in the ferromagnets. The mMTR arises from an interfacial temperature drop caused by magnon spin accumulations and can be engineered by the layer thicknesses, spin diffusion lengths, and spin conductances. The mMTR predicted here enables magnetothermal switching in insulator-based systems; we already predict large mMTR ratios up to 40% for superlattices of the electrically insulating magnet yttrium iron garnet and elemental metals.

Introduction.—The magneto-thermal resistance (MTR) effect enables the magnetic control of thermal transport. Solid-state devices with a high MTR ratio and a broad operating temperature range around room temperature are essential for thermal management technologies [1]. A traditional approach focuses on the MTR of single-phase bulk materials, but it often requires impractically high magnetic fields or extremely low operation temperatures [2–8]. More promising is the giant MTR in ferromagnetic (FM)|nonmagnetic (NM) multilayers [9–17], the thermal version of the giant magnetoresistance (GMR) [18, 19], where the thermal conductivity varies with the magnetization configurations of the ferromagnetic layers, opening a pathway towards nonvolatile, nanoscale thermal switching devices [20]. Similar to the essential role of electronic spin accumulation in the GMR, spin-dependent heat accumulation or temperature of electrons is proposed to explain the MTR in magnetic multilayers [15, 21]. Because of the Wiedemann-Franz law and short spin-dependent heat relaxation length (compared to the spin diffusion length), the MTR has long been considered a byproduct of the GMR and has only received little attention. Surprisingly, several experimental groups report an MTR exceeding the GMR [12, 13, 16, 17], implying an unconventional magneto-thermal transport mechanism.

Magnons, the collective quasi-particle excitations of magnetic order, serve as an additional carrier of energy and spin in a magnetic metal [22]. Under the gradient of a temperature or non-equilibrium magnon accumulation [23–25], magnon diffusion contributes to both heat and spin currents, leading to magnetic-field dependent thermal conduction [26–28] and the spin Seebeck effect [29],

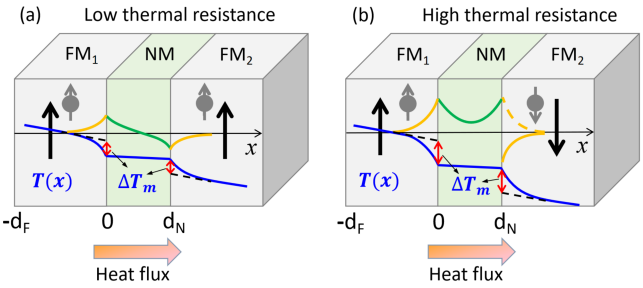

FIG. 1. Concept of the magnon-driven thermal resistance in (FM_1)|nonmagnetic metal (NM)|ferromagnet (FM_2). A thermal bias excites non-equilibrium magnon accumulations (orange solid curves). Its gradient generates a back-flow heat current by diffusion and thereby, for a fixed heat current bias, an additional temperature drop ΔT_m as sketched by the blue lines. (a) In the parallel configuration, the spin accumulations injected by the two FMs into the metal spacer cancel, corresponding to a high thermal conductance. In the antiparallel configuration (b), they add up to form a high-resistance state. The arrows on the grey dots represent the magnon spin angular momenta, the green solid curves in the NM layer the spin accumulation of electrons, and the dashed orange curves in (b) the magnonic spin accumulation opposite to the magnon number accumulation (solid orange curves).

respectively. Recently, Hirai *et al.* [30] reported surprisingly large magnon contributions to the thermal transport properties of a ferromagnetic metal even at room temperature.

Motivated by these experiments [17, 30] we present in this Letter a pronounced magnon-driven MTR (mMTR) in magnetic multilayers (see Fig. 1): a thermally driven magnon current within the FM layers produces non-equilibrium magnon accumulation near FM|NM interfaces that depends on the interlayer magnetic configuration and causes an additional temperature drop due

* tang.ping.a2@tohoku.ac.jp

to a feedback diffusion heat current, giving rise to the MTR effect. This is analogous to the GMR with current perpendicular to the interfaces, in which interfacial spin accumulation of electrons plays an essential role [31]. We explain the large mMTR at room temperature by two factors. While in the GMR only electrons near the Fermi level play a role, the boson statistics of magnons allow all of them to contribute to transport. Moreover, the magnon diffusion length can exceed that of the mobile electrons by orders of magnitude. Since magnons can exist in magnetic insulators, the mMTR goes beyond the GMR mechanism, offering the potential for insulator-based magnetothermal switching devices.

Model.—We address the mMTR for a spin valve of two identical FM layers and a thin NM spacer, as illustrated in Fig. 1, as well as FM|NM multilayers. In a metallic FM, both electrons and magnons contribute to the MTR. The electron-induced MTR is caused by spin-dependent thermal conductivities in the FM and FM|NM interfaces and thereby directly related to the GMR by the Wiedemann-Franz law. Here we focus on electrically insulting FM layers to isolate a previously unrecognized magnonic mechanism. Since the mMTR is caused by thermally excited (incoherent) magnons, we disregard the coherent magnon coupling between FM layers by a non-local exchange interaction through ultrathin metal spacers [32, 33], which may play a role in the mMTR only at low temperatures, viz. thermal energies of the order of the modified magnon gap.

In linear response a temperature (chemical potential) gradient ∂T_i ($\partial\mu_i$) drives spin [$\mathcal{J}_i$] and heat [Q_i] currents in the $i$the FM layer [25]

$$\begin{pmatrix} \frac{e}{\hbar}\mathcal{J}_i \\ Q_i \end{pmatrix} = -\begin{pmatrix} \sigma_m & \mathcal{L}_m \\ T_0\mathcal{L}_m & \kappa_F \end{pmatrix}\begin{pmatrix} \partial\mu_i/e \\ \partial T_i \end{pmatrix}, \tag{1}$$

where σ_m and $\mathcal{L}_m$ are the magnon spin conductivity and spin Seebeck coefficient, respectively, while κ_F is the total thermal conductivity including phonon contributions. We employed the Onsager reciprocity of the off-diagonal magnon Seebeck and Peltier coefficients at the average temperature T_0. The polarization of the magnon spin current in Eq. (1) is collinear with the magnetization direction of the ith FM layer and changes sign when reversing the magnetization. The spin [$\mathcal{J}_N$] and heat [Q_N] currents in the NM layer, on the other hand, obey

$$\begin{pmatrix} \mathcal{J}_N \\ Q_N \end{pmatrix} = -\begin{pmatrix} \frac{\hbar}{4e^2}\sigma_N & 0 \\ 0 & \kappa_N \end{pmatrix}\begin{pmatrix} \partial\mu_N \\ \partial T_N \end{pmatrix} \tag{2}$$

where σ_N and κ_N are the electric and thermal conductivities of the metal, respectively, and μ_N the spin chemical potential, *i.e.* the chemical potential difference of spin-up and -down electrons. In contrast to the FM layers, there are no off-diagonal elements.

Biasing the spin valve by a given heat current Q induces temperature and chemical potential gradients. Inverting the above relations

$$\partial T_i(x) = -\frac{Q}{\kappa_F} - \frac{T_0\mathcal{L}_m}{e\kappa_F}\partial\mu_i(x) \tag{3}$$

$$\partial T_N(x) = -\frac{Q}{\kappa_N}, \tag{4}$$

where magnon Peltier effect generates a non-equilibrium magnon accumulation and the second term in Eq. (3). The thermal resistivity ρ of the spin valve with spacer thickness d_N and equal thickness d_F of the two magnets reads

$$\rho \equiv \frac{\Delta T}{LQ} = \frac{1}{L}\left(\frac{2d_F}{\kappa_F} + \frac{d_N}{\kappa_N}\right) + \rho_m, \tag{5}$$

where $L = 2d_F + d_N$, ΔT is the total temperature drop. Here we introduced a magnon-driven magnetothermal resistivity $\rho_m = \Delta T_m/(LQ)$, where

$$\Delta T_m = \frac{T_0\mathcal{L}_m}{e\kappa_F}\int dx'[\partial\mu_1(x') + \partial\mu_2(x')] \tag{6}$$

is the temperature drop in the presence of a magnon accumulation. In the following, we calculate Eq. (6) and ρ_m by spin diffusion theory when the two magnetizations are parallel and antiparallel.

Results.—The solutions to the magnon diffusion equation $(\partial^2 - \lambda_m^{-2})\mu_i = 0$ are [23–25],

$$\mu_i(x) = A_i e^{x/\lambda_m} + B_i e^{-x/\lambda_m}, \tag{7}$$

where A_i and B_i are coefficients determined by boundary conditions and λ_m the magnon diffusion length. The electronic spin chemical potential in the NM layer obeys

$$\mu_N(x) = Ce^{x/\lambda_N} + De^{-x/\lambda_N} \tag{8}$$

where λ_N is the spin diffusion length of electrons. In a collinear configuration without interfacial spin torques, the spin currents at two NM-FM interfaces are conserved, *i.e.*

$$\mathcal{J}_1(0) = \mathcal{J}_N(0), \;\; \mathcal{J}_N(d_N) = s\mathcal{J}_2(d_N) \tag{9}$$

where $s = \pm$ accounts for the polarization of the magnonic spin current in the second FM layer, i.e., (+) when the magnetization of the second FM layer is aligned parallel (−) when antiparallel to that of the first FM layer. Assuming transparent NM|FM interfaces [34], the magnon and electron spin chemical potentials are also continuous at the interfaces with

$$\mu_1(0) = \mu_N(0), \;\; \mu_N(d_N) = s\mu_2(d_N) \tag{10}$$

where $s = -1$ reflects the annihilation of magnons in the second FM by a spin-flip in the normal metal when its magnetization is antiparallel, i.e., "magnon holes" with opposite spins are created in the second FM layer. When the FM thickness is smaller than or comparable to the magnon diffusion length we must specify the boundary

conditions at the outer interfaces. In the following, we consider several experimentally relevant cases.

(i) Spin-sinking contact. We first consider a spin valve sandwiched between good spin sinks such as Pt, which implies that $\mu_1(-d_F) = \mu_2(d_N+d_F) = 0$. The solution of Eq. (7) with these boundary conditions leads to thermal resistivities

$$\rho_m^{\rm P} = \frac{2\hbar}{e^2 L}\frac{T_0\mathcal{L}_m^2}{\kappa_F^2}\frac{G_m + G_N \tanh\frac{d_F}{\lambda_m}\tanh\frac{d_N}{2\lambda_N}}{\coth\frac{d_F}{\lambda_m}G_m^2 + \tanh\frac{d_F}{\lambda_m}G_N^2 + 2G_mG_N\coth\frac{d_N}{\lambda_N}} \tag{11}$$

$$\rho_m^{\rm AP} = \frac{2\hbar}{e^2 L}\frac{T_0\mathcal{L}_m^2}{\kappa_F^2}\frac{G_m + G_N \tanh\frac{d_F}{\lambda_m}\coth\frac{d_N}{2\lambda_N}}{\coth\frac{d_F}{\lambda_m}G_m^2 + \tanh\frac{d_F}{\lambda_m}G_N^2 + 2G_mG_N\coth\frac{d_N}{\lambda_N}} \tag{12}$$

TABLE I. The parameters for several normal metal spacers with long spin diffusion lengths at room temperature.

NM	σ_N(S/μm)	κ_N(W/(K·m))	λ_N(nm)	$G_N(10^{16}\,\mathrm{m}^{-2})$
Al	31	237	600 [35]	5
Cu	35	401	350 [36]	10
Au	19	318	60 [37]	32

for the parallel and antiparallel configurations, respectively. Here $G_m \equiv (\hbar/e^2)\bar{\sigma}_m/\lambda_m$ and $G_N \equiv (\hbar/4e^2)\sigma_N/\lambda_N$ are the spin conductances (per unit area) in the FM and NM, respectively, and

$$\bar{\sigma}_m \equiv \sigma_m\left(1 - \frac{T_0\mathcal{L}_m^2}{\kappa_F\sigma_m}\right) = \sigma_m\left(1 - zT_m\frac{\kappa_m}{\kappa_F}\right) \tag{13}$$

is the magnon spin conductivity corrected for the spin Seebeck/Peltier effects, where $zT_m \equiv T_0\mathcal{L}_m^2/(\kappa_m\sigma_m)$ is a thermomagnonic figure of merit and κ_m the magnon thermal conductivity. Here $\rho_m^{\rm P}$ and $\rho_m^{\rm AP}$ scale as κ_F^{-2}, implying that they can be enhanced by choosing FM layers with low thermal conductivities.

We measure the heat-valve performance by the mMTR ratio $(\rho^{\rm AP} - \rho^{\rm P})/\rho^{\rm P}$

$$\mathrm{mMTR} = \frac{\eta}{\frac{2d_F}{\lambda_m} + \frac{\kappa_F}{\kappa_N}\frac{d_N}{\lambda_m} + 2\eta\frac{1+\xi\tanh\frac{d_F}{\lambda_m}\tanh\frac{d_N}{2\lambda_N}}{\coth\frac{d_F}{\lambda_m}+2\xi\coth\frac{d_N}{\lambda_N}+\xi^2\tanh\frac{d_F}{\lambda_m}}} \times \frac{4\xi\tanh^2\frac{d_F}{\lambda_m}\mathrm{csch}\frac{d_N}{\lambda_N}}{1 + 2\xi\tanh\frac{d_F}{\lambda_m}\coth\frac{d_N}{\lambda_N} + \xi^2\tanh^2\frac{d_F}{\lambda_m}}, \tag{14}$$

where $\xi = G_N/G_m$ is the ratio of the spin conductances of electrons to magnons and

$$\eta = zT_m\frac{\kappa_m}{\kappa_F}\left(1 - zT_m\frac{\kappa_m}{\kappa_F}\right)^{-1} \tag{15}$$

is another dimensionless figure of merit that measures the impact of a magnon accumulation on the thermal conductivity. According to Eq. (14), η, ξ and the normalized thicknesses of the NM and FM layers govern the magnitude of the mMTR that increases monotonically with increasing η or decreasing d_N/λ_N, but decreases for large d_F/λ_m and ξ. In Fig. 2(a) and (b) we tune the parameters to maximize the effect. When $d_N \ll \lambda_N$, the mMTR ratio approaches a ξ-independent maximum value

$$\mathrm{mMTR} \overset{d_N\ll\lambda_N}{\to} \frac{\eta}{1+\frac{R_N}{R_F}}\frac{\lambda_m}{d_F}\tanh\frac{d_F}{\lambda_m} \tag{16}$$

where $R_N = d_N/\kappa_N$ and $R_F = 2d_F/\kappa_F$ are the thermal resistances in the absence of the magnon accumulation

(ii) Zero spin current. When the spin valve is sandwiched by nonmagnetic insulators (e.g., MgO), the magnon spin currents at the outer interfaces of two FM

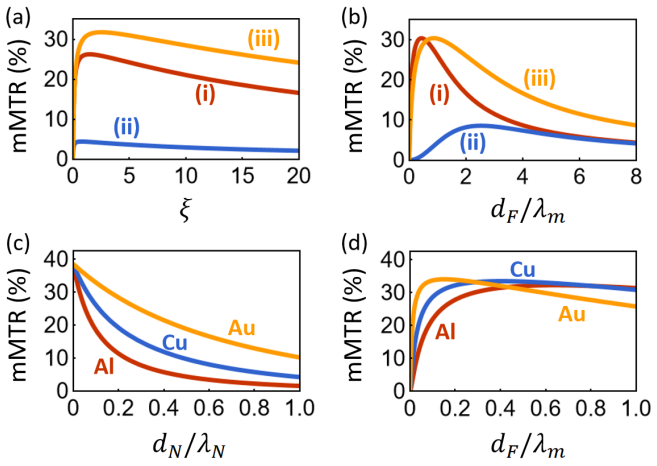

FIG. 2. (a) and (b): The mMTR ratio as a function of ξ and d_F/λ_m of a YIG|NM|YIG spin valve calculated for outer boundary conditions corresponding to an (i) ideal spin sink, (ii) zero spin current, and (iii) a superlattice stack. Here $d_F/\lambda_m = 1$ and $d_N/\lambda_N = 0.1$ in (a), and $d_N/\lambda_N = 0.1$ and $\kappa_F\lambda_N/(\kappa_N\lambda_m) = 0.01$ in (b). (c) and (d): mMTR dependence on FM and NM thicknesses in a [FM|NM] superlattice with different NMs with $d_F/\lambda_F = 0.1$ in (c) and $d_N/\lambda_N = 0.1$ in (d).

layers vanish, leading to

$$\mathrm{mMTR} = \frac{\eta}{\frac{2d_F}{\lambda_m} + \frac{\kappa_F}{\kappa_N}\frac{d_N}{\lambda_m} + 2\eta\frac{2\tanh\frac{d_F}{2\lambda_m}+\xi\coth\frac{d_N}{2\lambda_N}}{1+\xi\coth\frac{d_F}{\lambda_m}\coth\frac{d_N}{2\lambda_N}}} \times \frac{2\xi\mathrm{csch}^2\frac{d_N}{2\lambda_N}\tanh^2\frac{d_F}{2\lambda_m}}{(\xi\coth\frac{d_F}{\lambda_m}+\coth\frac{d_N}{2\lambda_N})(1+\xi\coth\frac{d_F}{\lambda_m}\coth\frac{d_N}{2\lambda_N})} \overset{d_N\ll\lambda_N}{\to} \frac{\eta\frac{\lambda_m}{d_F}\tanh^2\frac{d_F}{2\lambda_m}\tanh\frac{d_F}{\lambda_m}}{1+\frac{R_N}{R_F}+\eta\frac{\lambda_m}{d_F}\tanh\frac{d_F}{\lambda_m}}, \quad (17)$$

which agrees with Eq. (14) in the limit of $d_F/\lambda_m \gg 1$, as expected. However, an FM thickness comparable to λ_m suppressed the effect [Fig. 2(b)] because the magnon accumulation near the outer interfaces compensates for the ones near the FM|NM interfaces.

(iii) Superlattice condition. In a spin valve embedded in a magnetic superlattice with [FM|NM] unit cell, the same surroundings for two interfaces of each FM layer correspond to outer boundary conditions when the magnon chemical potentials at the outer boundary are opposite to the ones at the FM|NM interfaces, i.e., $\mu_1(-d_F) = -\mu_1(0)$ and $\mu_2(d_N) = -\mu_2(d_N + d_F)$.

$$\mathrm{mMTR} = \frac{\eta}{\frac{2d_F}{\lambda_m} + \frac{\kappa_F}{\kappa_N}\frac{d_N}{\lambda_m} + 4\eta\frac{\tanh\frac{d_F}{2\lambda_m}}{1+\xi\coth\frac{d_N}{2\lambda_N}\tanh\frac{d_F}{2\lambda_m}}} \frac{8\xi\tanh^2\frac{d_F}{2\lambda_m}\mathrm{csch}\frac{d_N}{\lambda_N}}{(1+\xi\tanh\frac{d_F}{2\lambda_m}\tanh\frac{d_N}{2\lambda_N})(1+\xi\tanh\frac{d_F}{2\lambda_m}\coth\frac{d_N}{2\lambda_N})} \overset{d_N\ll\lambda_N}{\to} \frac{2\eta}{1+\frac{R_N}{R_F}}\frac{\lambda_m}{d_F}\tanh\frac{d_F}{2\lambda_m}. \quad (18)$$

Since the magnon accumulation near both two interfaces of each FM layer contributes to the magnetothermal transport, the mMTR is enhanced compared to the previous cases [Fig. 2(a) and (b)], in the limit of $d_N \ll \lambda_N$ and $d_F \gg \lambda_m$ the mMTR becomes two times larger than Eq. (16). A similar enhancement of the spin Seebeck effect has been reported in metallic magnetic multilayers [38].

Let us consider a specific spin valve composed of NM (= Al, Cu, Au) and the magnetic insulator yttrium iron garnet (YIG) with well-known parameters at room temperature ($T_0 = 300\,\mathrm{K}$): $\sigma_m = 5\times10^5\,\mathrm{S/m}$ [25], $\mathcal{L}_m/\sigma_m = 110\,\mu\mathrm{V/K}$ [39] and $\lambda_m = 70\,\mathrm{nm}$ [40], $\kappa_{\mathrm{YIG}} = 6.6\,\mathrm{W/(K\cdot m)}$ [41], which gives $\eta = 0.38$ and $G_m = 2.12\times10^{16}\,\mathrm{m}^{-2}$. Table I summarizes the relevant parameters for Al, Cu, and Au. Fig. 2(a) and (b) plots the mMTR ratio as a function of ξ and d_F/λ_m for the aforementioned outer boundary conditions, respectively. Fig. 2(c) and (d) shows the mMTR with the superlattice boundary condition for Al, Cu, and Au spacers as a function of the FM and NM thicknesses, respectively. The mMTR decreases monotonically with the NM thickness; it is largest ($\sim\eta$) at an optimal thickness of the FM that is much smaller than its magnon diffusion length, approaching zero when $\kappa_F d_N/(\kappa_N\lambda_m) \to 0$.

Conclusion.—We predict a substantial room-temperature mMTR in spin valves with electrically insulating FM layers. We trace its origin to an interfacial temperature drop caused by a non-equilibrium magnon spin accumulation that depends on the relative orientation between two FM layers. The mMTR ratio can be engineered by the spin conductances, boundary conditions, and layer thicknesses. Our results may explain the giant MTR ratio in metallic multilayers [17]. One might consider simply adding the electronic and magnonic contributions to the MTR. Indeed, magnons contribute to a large MTR but suppress the GMR [42], which might partly explain the observations. However, a thorough treatment requires better knowledge of the magnon transport parameters in ferromagnetic metals and the inclusion of the magnon-electron drag effect [42–46].

Acknowledgment.—The authors thank Y. Sakuraba, T. Hirai, F. Makino, and A. O. Leon for valuable discussions. P.T., K.U., and G.E.W.B. were supported by Grant-in-Aid for Scientific Research (S) (No. 22H04965) from JSPS KAKENHI, Japan. P. T. was also supported by Grant-in-Aid for Early-Career Scientists (No. 23K13050), K.U. by ERATO "Magnetic Thermal Management Materials Project" (No. JPMJER2201) from JST, Japan, and G.E.W.B. by JSPS KAKENHI Grants (Nos. 19H00645 and 24H02231).

[1] A. L. Moore and L. Shi, Emerging challenges and materials for thermal management of electronics, Materials Today **17**, 163 (2014).
[2] B. Chen, A. G. Rojo, C. Uher, H. L. Ju, and R. L. Greene, Magnetothermal conductivity of $la_{0.8}ca_{0.2}mno_3$, Physical Review B **55**, 15471 (1997).
[3] B. Zhang, X. Zhang, S. Yu, J. Chen, Z. Cao, and G. Wu, Giant magnetothermal conductivity in the ni–mn–in ferromagnetic shape memory alloys, Applied Physics Letters **91** (2007).
[4] X. F. Sun, A. A. Taskin, X. Zhao, A. N. Lavrov, and Y. Ando, Large magnetothermal conductivity in $GdBaCo_2O_{5+x}$ single crystals, Physical Review B **77**, 054436 (2008).
[5] X. Wang, C. Fan, Z. Zhao, W. Tao, X. Liu, W. Ke, X. Zhao, and X. Sun, Large magnetothermal conductivity of homno 3 single crystals and its relation to the magnetic-field-induced transitions of magnetic structure, Physical Review B **82**, 094405 (2010).
[6] C. Fu, S. N. Guin, T. Scaffidi, Y. Sun, R. Saha, S. J. Watzman, A. K. Srivastava, G. Li, W. Schnelle, S. S. Parkin, *et al.*, Largely suppressed magneto-thermal con-

ductivity and enhanced magneto-thermoelectric properties in $PtSn_4$, Research **2020**, 8 (2020).
[7] K. Hirata, K. Kuga, M. Matsunami, M. Zhu, J. P. Heremans, and T. Takeuchi, Magneto-thermal conductivity effect and enhanced thermoelectric figure of merit in Ag_2Te, AIP Advances **13** (2023).
[8] K. G. Koster, J. Hise, J. P. Heremans, and J. E. Goldberger, Giant magnetothermal conductivity switching in semimetallic WSi_2 single crystals, ACS Applied Electronic Materials **6**, 1757 (2024).
[9] H. Sato, Y. Aoki, Y. Kobayashi, H. Yamamoto, and T. Shinjo, Giant magnetic field effect on thermal conductivity of magnetic multilayers, cu/co/cu/ni (fe), Journal of the Physical Society of Japan **62**, 431 (1993).
[10] H. Sato, Y. Aoki, Y. Kobayashi, H. Yamamoto, and T. Shinjo, Huge magnetic field-dependent thermal conductivity in magnetic multilayer films, Journal of Magnetism and Magnetic Materials **126**, 410 (1993).
[11] J. Shi, K. Pettit, E. Kita, S. S. P. Parkin, R. Nakatani, and M. B. Salamon, Field-dependent thermoelectric power and thermal conductivity in multilayered and granular giant magnetoresistive systems, Physical Review B **54**, 15273 (1996).
[12] Y. Yang and M. Asheghi, Thermal characterization of Cu/CoFe multilayer for giant magnetoresistive (gmr) head applications, in *ASME International Mechanical Engineering Congress and Exposition*, Vol. 4711 (2004) pp. 199–210.
[13] T. Jeong, M. T. Moneck, and J.-G. Zhu, Giant magnetothermal conductivity in magnetic multilayers, IEEE Transactions on Magnetics **48**, 3031 (2012).
[14] J. Kimling, K. Nielsch, K. Rott, and G. Reiss, Field-dependent thermal conductivity and lorenz number in co/cu multilayers, Physical Review B **87**, 134406 (2013).
[15] J. Kimling, R. Wilson, K. Rott, J. Kimling, G. Reiss, and D. G. Cahill, Spin-dependent thermal transport perpendicular to the planes of co/cu multilayers, Physical Review B **91**, 144405 (2015).
[16] N. Asam, K. Yamanoi, K. Ohnishi, and T. Kimura, Thermal spin-valve effect in magnetic multi-layered nanowires, Journal of Superconductivity and Novel Magnetism **32**, 3109 (2019).
[17] H. Nakayama, B. Xu, S. Iwamoto, K. Yamamoto, R. Iguchi, A. Miura, T. Hirai, Y. Miura, Y. Sakuraba, J. Shiomi, *et al.*, Above-room-temperature giant thermal conductivity switching in spintronic multilayers, Applied Physics Letters **118** (2021).
[18] M. N. Baibich, J. M. Broto, A. Fert, F. N. Van Dau, F. Petroff, P. Etienne, G. Creuzet, A. Friederich, and J. Chazelas, Giant magnetoresistance of (001)Fe/(001)Cr magnetic superlattices, Physical Review Letters **61**, 2472 (1988).
[19] G. Binasch, P. Grünberg, F. Saurenbach, and W. Zinn, Enhanced magnetoresistance in layered magnetic structures with antiferromagnetic interlayer exchange, Physical Review B **39**, 4828 (1989).
[20] H. Arima, M. R. Kasem, H. Sepehri-Amin, F. Ando, K.-i. Uchida, Y. Kinoshita, M. Tokunaga, and Y. Mizuguchi, Observation of nonvolatile magneto-thermal switching in superconductors, Communications Materials **5**, 34 (2024).
[21] F. Dejene, J. Flipse, G. Bauer, and B. Van Wees, Spin heat accumulation and spin-dependent temperatures in nanopillar spin valves, Nature Physics **9**, 636 (2013).
[22] T. An, V. Vasyuchka, K. Uchida, A. Chumak, K. Yamaguchi, K. Harii, J. Ohe, M. Jungfleisch, Y. Kajiwara, H. Adachi, *et al.*, Unidirectional spin-wave heat conveyer, Nature Materials **12**, 549 (2013).
[23] S. S.-L. Zhang and S. Zhang, Magnon mediated electric current drag across a ferromagnetic insulator layer, Physical Review Letters **109**, 096603 (2012).
[24] S. Rezende, R. Rodríguez-Suárez, R. Cunha, A. Rodrigues, F. Machado, G. Fonseca Guerra, J. Lopez Ortiz, and A. Azevedo, Magnon spin-current theory for the longitudinal spin-seebeck effect, Physical Review B **89**, 014416 (2014).
[25] L. J. Cornelissen, K. J. Peters, G. E. Bauer, R. Duine, and B. J. van Wees, Magnon spin transport driven by the magnon chemical potential in a magnetic insulator, Physical Review B **94**, 014412 (2016).
[26] W. B. Yelon and L. Berger, Magnon heat conduction and magnon scattering processes in fe-ni alloys, Physical Review B **6**, 1974 (1972).
[27] Y. Hsu and L. Berger, Magnon heat conduction and magnon lifetimes in the metallic ferromagnet $fe_{68}co_{32}$ at low temperatures, Physical Review B **14**, 4059 (1976).
[28] S. Rezende and J. Lopez Ortiz, Thermal properties of magnons in yttrium iron garnet at elevated magnetic fields, Physical Review B **91**, 104416 (2015).
[29] K. Uchida, J. Xiao, H. Adachi, J.-i. Ohe, S. Takahashi, J. Ieda, T. Ota, Y. Kajiwara, H. Umezawa, H. Kawai, *et al.*, Spin seebeck insulator, Nature Materials **9**, 894 (2010).
[30] T. Hirai, T. Morita, S. Biswas, J. Uzuhashi, T. Yagi, Y. Yamashita, V. K. Kumar, F. Makino, R. Modak, Y. Sakuraba, *et al.*, Nonequilibrium magnonic thermal transport engineering, arXiv preprint arXiv:2403.04166 (2024).
[31] M. A. Gijs and G. E. Bauer, Perpendicular giant magnetoresistance of magnetic multilayers, Advances in Physics **46**, 285 (1997).
[32] A. Ganguly and C. Vittoria, Magnetostatic wave propagation in double layers of magnetically anisotropic slabs, Journal of Applied Physics **45**, 4665 (1974).
[33] H. Sasaki and N. Mikoshiba, Directional coupling of magnetostatic surface waves in a layered structure of yig films, Journal of Applied Physics **52**, 3546 (1981).
[34] This assumption is justified when the bulk spin and magnon resistances are much larger than those of the interfaces. For the interface of YIG and typical normal metals (e.g., Au, Pt), the interfacial spin conductance governed by the spin mixing conductance is of the order 10^{18}-$10^{19}\,\mathrm{m}^{-2}$ [47], which is around two orders of magnitude of larger than bulk spin conductances.
[35] F. J. Jedema, M. S. Nijboer, A. T. Filip, and B. J. van Wees, Spin injection and spin accumulation in all-metal mesoscopic spin valves, Physical Review B **67**, 085319 (2003).
[36] F. J. Jedema, A. Filip, and B. Van Wees, Electrical spin injection and accumulation at room temperature in an all-metal mesoscopic spin valve, Nature **410**, 345 (2001).
[37] T. Kimura, J. Hamrle, and Y. Otani, Estimation of spin-diffusion length from the magnitude of spin-current absorption: Multiterminal ferromagnetic/nonferromagnetic hybrid structures, Physical Review B **72**, 014461 (2005).
[38] R. Ramos, T. Kikkawa, M. H. Aguirre, I. Lucas, A. Anadón, T. Oyake, K. Uchida, H. Adachi, J. Shiomi, P. A. Algarabel, L. Morellón, S. Maekawa, E. Saitoh,

and M. R. Ibarra, Unconventional scaling and significant enhancement of the spin seebeck effect in multilayers, Physical Review B **92**, 220407 (2015).

[39] According to the Boltzmann transport approach, $\sigma_m = \frac{e^2\tau}{3}\int \frac{d\mathbf{k}}{(2\pi)^3} v_{\mathbf{k}}^2 \frac{\partial n}{\partial \varepsilon_{\mathbf{k}}}$ and $\mathcal{L}_m = \frac{e\tau}{3}\int \frac{d\mathbf{k}}{(2\pi)^3} v_{\mathbf{k}}^2 \frac{\partial n}{\partial T}$, where $n(\varepsilon_{\mathbf{k}})$ is the magnon equilibrium distribution with energy $\varepsilon_{\mathbf{k}}$, and τ and $\mathbf{v_k}$ are the magnon constant relaxation time and group velocity, respectively. Adopting the relevant parameters for the magnon dispersion in Ref. [25] leads to $\mathcal{L}_m/\sigma_m = 110\,\mu$V, which is around two orders of magnitude larger than the electronic Seebeck coefficient in common metals.

[40] We adopt the magnon diffusion length in Ref. [24] for a perpendicular stack of YIG with nonmagnetic metals, rather than the one in Ref. [48] obtained from the nonlocal magnon transport.

[41] F. Mohmed, F. A. Dar, S. Rubab, M. Hussain, and L.-Y. Hua, Magnetic and thermal properties of ferromagnetic insulator: Yttrium iron garnet, Ceramics International **45**, 2418 (2019).

[42] Y. Cheng, K. Chen, and S. Zhang, Interplay of magnon and electron currents in magnetic heterostructure, Physical Review B **96**, 024449 (2017).

[43] F. J. Blatt, D. J. Flood, V. Rowe, P. A. Schroeder, and J. E. Cox, Magnon-drag thermopower in iron, Physical Review Letters **18**, 395 (1967).

[44] G. N. Grannemann and L. Berger, Magnon-drag peltier effect in a ni-cu alloy, Physical Review B **13**, 2072 (1976).

[45] M. V. Costache, G. Bridoux, I. Neumann, and S. O. Valenzuela, Magnon-drag thermopile, Nature Materials **11**, 199 (2012).

[46] S. J. Watzman, R. A. Duine, Y. Tserkovnyak, S. R. Boona, H. Jin, A. Prakash, Y. Zheng, and J. P. Heremans, Magnon-drag thermopower and nernst coefficient in fe, co, and ni, Physical Review B **94**, 144407 (2016).

[47] M. Haertinger, C. H. Back, J. Lotze, M. Weiler, S. Geprägs, H. Huebl, S. T. B. Goennenwein, and G. Woltersdorf, Spin pumping in yig/pt bilayers as a function of layer thickness, Physical Review B **92**, 054437 (2015).

[48] L. Cornelissen, J. Liu, R. Duine, J. B. Youssef, and B. Van Wees, Long-distance transport of magnon spin information in a magnetic insulator at room temperature, Nature Physics **11**, 1022 (2015).